diffusion-fundamentals

The Open-Access Journal for the Basic Principles of Diffusion Theory, Experiment and Application

MATHEMATICAL MODELING AND VISUALIZATION OF GAS TRANSPORT IN A ZEOLITE BED USING A SLICE SELECTION PROCEDURE

M. Petryk[1], S. Leclerc[2,3], D. Canet[2], J. Fraissard[4,5]

[1]Modélisation du Transfert de Masse en Milieu Hétérogène et Nanoporeux, Université Technique d'Etat Ivan Pul'uy, Ternopil, 46001 Ukraine; E-mail : Mykhaylo_Petryk@tu.edu.te.ua
[2]Méthodologie RMN, UMR 7565 CNRS - Nancy Université, 54506 Vandoeuvre-les-Nancy Cedex, France
[3]LEMTA, UMR 7563 CNRS - Nancy Université, 54504 Vandoeuvre-les-Nancy Cedex, France
[4]Physique Quantique, ESPCI, 10 rue Vauquelin, 75231 Paris Cedex 05, France
[5]Université P. et M. Curie, 4 place Jussieu, 75252 Paris Cedex 05, France; E-mail jfr@ccr.jussieu.fr

Summary

We present the analytical solution of the equations of gas diffusion in a heterogeneous zeolite bed. The problem is handled by assuming that the bed consists of a large number of very thin layers of solid, perpendicular to the direction of propagation of the gas. Mass transfer by diffusion in such a material is determined by a system of differential equations with boundary and interface conditions. The results allow the theoretical determination of the time dependence of the concentration profiles and the inter- and intra-crystallite diffusion coefficients of a gas in each layer of the bed. A numerical application concerns the diffusion of benzene in a cylindrical bed of ZSM5 displaced vertically and rapidly, step by step, inside the NMR probe. Thus we can obtain the time dependence of the concentration of gas absorbed at the level of each slice. These coupled investigations give a better understanding of the diffusion process in this multilayer material.

Introduction.

Mathematical modeling of mass transfer by diffusion in zeolite beds or other solids and the methods for finding the analytical solutions have been extensively studied by several authors [1-19]. Molecular transport in a bed of zeolite involves two processes: diffusion in the macropores formed by the space between the crystallites (intercrystallite diffusion) and diffusion in the micropores within the crystallites (intracrystallite diffusion). To determine the contribution of each of these processes to the overall diffusion process, one has to know the values of certain parameters, such as the pressure in the gas phase, the dimensions of the crystallite bed, the adsorption isotherms, etc. In the present work we assume that the bed consists of a large number of very thin layers of solid perpendicular to the direction of propagation of the gas.

As an application of the theoretical results we present the results of a study dealing with the penetration of a gas (benzene) in a zeolite catalyst (ZSM5) bed using the technique described in [20]. The proposed experimental method relies on the vertical displacement, step by step, of the bed during the adsorption of the gas, the NMR detection using a very thin coil. In this way, the region effectively probed is limited to a very thin slice. Thus we can obtain the variation as a function of time of the concentration of gas absorbed at the level of each slice.

This dual approach enables us for the first time to determine the diffusion coefficient profiles at every position in the bed.

Experiments

NMR apparatus.

Our aim is to determine the evolution of the NMR spectrum along the length of a heterogeneous sample in the z direction of the magnetic field B_0. This original method of imaging has been presented in ref. 20.

The idea is to select successively several sections at different positions of the sample along the z axis (Fig. 1). In this way one obtains for each position a spectrum corresponding to the composition of the sample at this point, which proves to be very interesting in the case of heterogeneous samples, and especially for the diffusion of gas before adsorption equilibrium. In order to perform these experiments a device was designed to displace the sample in the magnet Although this device allows sample displacements as low as 1 μm, in a classical experiment one uses more reasonably a 50 or 100 μm step, i.e. a value considerably less than that of the section chosen, which is generally between 0.5 and 2 mm. The spectrum obtained corresponds therefore to the overlapping of 10 to 20 elementary sections (by elementary section we mean a section of thickness equal to the step). To treat this problem an algorithm has been developed [20] which is designed to reconstruct the spectrum corresponding to each elementary section from the spectra measured for all the sample positions.

After testing this method with the help of different samples, including the study of solvent penetration into multilayer polymeric materials [20], we have applied it to the kinetics of the adsorption of gaseous benzene in a zeolite.

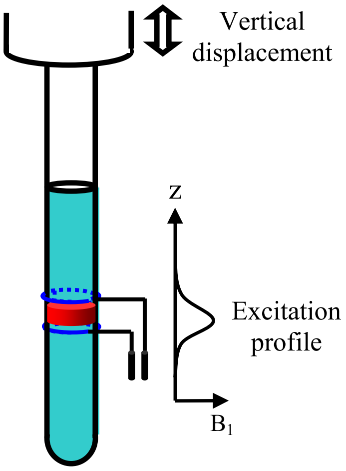

Fig. 1: Principle of experiment

Blue: sample; Red: zone of excitation

Adsorption measurement

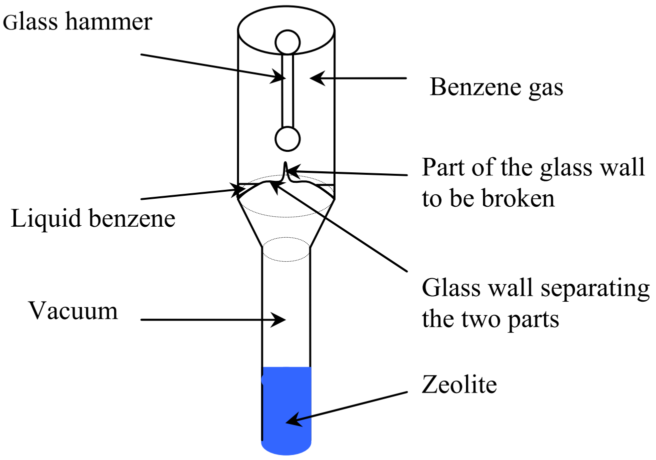

Fig. 2: Experimental set-up

The gas to be adsorbed is in equilibrium with the liquid, in the upper part of the ampule. (Fig. 2). It begins to diffuse into the zeolite bed when the wall separating the two parts is broken by means of the glass hammer. In accordance with the principle mentioned above, the zeolite sample is displaced vertically in the magnet during the adsorption, a few microns at a time. The signal of the gas is detected for each position, rapidly so as to obtain the best possible precision. When the sample reaches the uppermost or lowest position it starts again in the opposite direction, and continues in this way until adsorption equilibrium is reached. By this means one obtains a curve of gas adsorption as a function of time for each level in the adsorbent.

In the present case we have studied the adsorption of benzene at 25°C in a 15 mm-deep bed of ZSM5 zeolite. In the upper part of the ampule the vapor pressure of benzene corresponds to the saturation vapor pressure in equilibrium with the liquid at 25°C.

Mathematical modeling

The model developed here is analogous to the bipore model developed in references [2-12, 15-19, 21,22] . A cylindrical bed of microporous zeolite crystallites, assumed to be spherical (radius R), is exposed to a constant concentration of adsorbate in the gas phase (Fig. 2 and 3). One face of this bed is permeable to the gas. In this case one can consider that gas diffusion is linear in the macropores (*z* direction along the height, l, of the bed) and radial in the micropores. We assume that the zeolite bed consists of a large number, n, of very thin layers of solid, of thickness $\Delta l_k = l_{k+1} - l_k$, perpendicular to the propagation of the gas in the *z* direction. We have made the following assumptions: *i*) during the evolution of the system towards equilibrium there has to be a concentration gradient in the macropores and/or in the micropores; *ii*) the effect of heat is negligible; *iii*) diffusion occurs in the Henry's law region of the adsorption isotherm.

The mathematical model of gas diffusion kinetics in the zeolite bed (which we consider to be a heterogeneous and multilayer porous medium) is defined by the solutions of the system of differential equations:

$$\varepsilon_{inter,k} \frac{\partial c_k}{\partial t} = D_{inter,k} \cdot \varepsilon_{inter,k} \frac{\partial^2 c_k}{\partial z^2} - \frac{3\left(1-\varepsilon_{inter,k}\right)}{R} \cdot \left(D_{intra,k} \frac{\partial q_k}{\partial r}\right)\Big|_{r=R} \quad ; \tag{1}$$

$$\frac{\partial q_k}{\partial t} = D_{intra,k}\left(\frac{\partial^2 q_k}{\partial r^2} + \frac{2}{r}\frac{\partial q_k}{\partial r}\right) \tag{2}$$

in the domains $I_n = \left\{ t > 0, r \in \left(0,R\right), z \in \bigcup\limits_{k=1}^{n+1} \left(l_{k-1}, l_k\right); l_0 = 0; l_{n+1} \equiv l < \infty \right\}$ corresponding to the mass balance in the macropores (c_k) and in the micropores (q_k) for each k layer. The meaning of all notations is given in the Nomenclature Section.

With the initial conditions:

$$c_k\left(t=0,z\right) = 0, \quad q_k\left(t=0,r,z\right) = 0 ; \tag{3}$$

the boundary conditions:

$$c_{n+1}\left(t, z = l\right) = c_{\infty\, n+1}, \quad q_k\left(t, r = R, z\right) = K_k \cdot c_k\left(z,t\right); \tag{4}$$

$$\frac{\partial c_1}{\partial z}\left(t, z = 0\right) = 0, \quad \frac{\partial q_k\left(t, r = 0, z\right)}{\partial r} = 0 \tag{5}$$

and the interface conditions between adjacent layers along the z axis:

$$\left[c_k(t,z) - c_{k+1}(t,z)\right]\Big|_{z=l_k} = 0; \left[\frac{\partial}{\partial z}c_k(t,z) - \frac{\partial}{\partial z}c_{k+1}(t,z)\right]\Big|_{z=l_k} = 0,\ k = \overline{1,n} \tag{6}$$

where $K_k = \dfrac{q_{\infty_k}}{c_{\infty_k}}; k = \overline{1, n+1}$.

Using dimensionless quantities (except time),

$$C_k = \frac{c_k}{c_{\infty_k}}; \qquad Q_k = \frac{q_k}{q_{\infty_k}}; \qquad Z = \frac{z}{l}; \qquad X = \frac{r}{R}, \qquad L_k = \frac{l_k}{l}$$

in Eqs. (1) and (2) the problem becomes: to find the solution of the partial differential equations:

$$\tau_{M_k} \cdot \frac{\partial C_k}{\partial t} = \frac{\partial^2 C_k}{\partial Z^2} - \Gamma_k \frac{\partial Q_k}{\partial X}\Big|_{X=1}; \tag{7}$$

$$\tau_{m_k} \cdot \frac{\partial Q_k}{\partial t} = \frac{\partial^2 Q_k}{\partial X^2} + \frac{2}{X}\frac{\partial Q_k}{\partial X}; \tag{8}$$

in the domain: $D_n = \left\{ t > 0, X \in (0,1), Z \in \bigcup_{k=1}^{n+1} (L_{k-1}, L_k); L_0 = 0; L_{n+1} \equiv 1 \right\}$

with the initial conditions:

$$C_k(t=0,Z) = 0, \qquad Q_k(t=0,X,Z) = 0; \tag{9}$$

the boundary conditions:

$$C_{n+1}(t,Z=1) = 1 \;; \qquad Q_k(t,X=1,Z) = C_k(t,Z); \tag{10}$$

$$\frac{\partial C_1}{\partial Z}(t,Z=0) = 0 \;; \quad \frac{\partial Q_k}{\partial X}(t,X=0,Z) = 0 \tag{11}$$

and interface conditions:

$$\left[C_k(t,Z) - C_{k+1}(t,Z) \right]\big|_{Z=L_k} = 0; \left[\frac{\partial}{\partial Z} C_k(t,Z) - \frac{\partial}{\partial Z} C_{k+1}(t,Z) \right]\big|_{Z=L_k} = 0; k = \overline{1,n}; \tag{12}$$

here: $\Gamma_k = \dfrac{3}{P_{inter_k}} \cdot \dfrac{\tau_{M_k}}{\tau_{m_k}}$; $\tau_{M_k} = \dfrac{l^2}{D_{inter_k}}$; $\tau_{m_k} = \dfrac{R^2}{D_{intra_k}}$;

$$P_{inter_k} = \frac{\varepsilon_{inter_k} \cdot C_k}{\varepsilon_{inter_k} \cdot C_k + \left(1 - \varepsilon_{inter_k} \cdot C_k\right) \cdot Q_k} \approx \frac{\varepsilon_{inter_k}}{\varepsilon_{inter_k} + \left(1 - \varepsilon_{inter_k}\right) \cdot \dfrac{Q_k}{C_k}}, k = \overline{1, n+1}.$$

The adsorption constant K_k of molecules (for example, hydrocarbons) in zeolites is usually very high. Therefore ε_{inter} is much smaller than (1 - ε_{inter}) K and can be neglected in the expression of $P_{inter,,k}$ giving the relative amount of gas in the intercrystallite space ΔL_k .

$$P_{inter_k} = \frac{\varepsilon_{inter_k}}{\left(1 - \varepsilon_{inter_k}\right) \cdot K_k}, k = \overline{1, n+1} \cdot$$

If $\tau_{m,k} >> \tau_{M,k}$, $\Gamma_k << 1$, the process in the layer ΔL_k is controlled by intracrystallite diffusion. It is the opposite if $\tau_{M,k} >> \tau_{m,k}$ ($\Gamma_k >> 1$). If $\Gamma_k \approx 1$, inter- and intracrystallite diffusions should control the overall diffusion in such a layer [9].

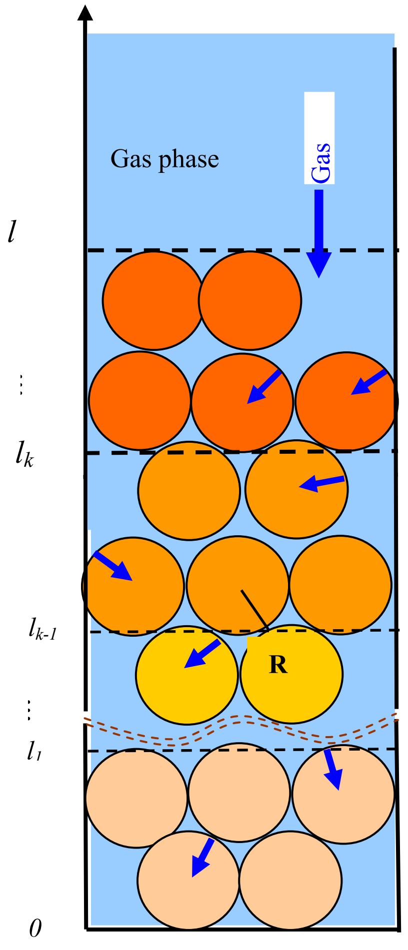

Diffusion in macropores

Length of the bed: l
Characteristic position of the layer: l_k, , $k=\overline{1,n+1}$
Thickness of layer k: $\Delta l_k = l_{k+1} - l_k$, $k=\overline{1,n+1}$
Intercrystallite diffusion coefficient in k layer: $D_{inter,k}$;
Corresponding characteristic time: $\tau_{inter,k}$
In the theoretical part, l is the top of the bed and 0 is the bottom.

Diffusion in micropores

Crystallite diameter: R
Intracrystallite diffusion coefficient in the k layer: $D_{intra,k}$
Corresponding characteristic time: $\tau_{intra,\,k}$
In the theoretical part, r = 0 corresponds to the center of the sphere.

$l >> R$; $D_{inter,k} >> D_{intra,k}$; $k=\overline{1,n+1}$

Figure 3. The process of diffusion in the zeolite bed

Putting $Q_k = \dfrac{N_k}{X}$, $k=\overline{1,n+1}$ into Eqs. (7)-(12), the system becomes:

$$\tau_{M,\kappa}\frac{\partial C_\kappa}{\partial t} = \frac{\partial^2 C_\kappa}{\partial Z^2} - \Gamma_k \left(\frac{1}{X}\frac{\partial N_k}{\partial X} - \frac{1}{X^2} N_k \right)\bigg|_{X=1} \equiv \frac{\partial^2 C_k}{\partial Z^2} - \left[\frac{\partial N_k}{\partial X} - N \right]_{X=1}, \tag{13}$$

$$\tau_{m,\kappa}\frac{\partial N_\kappa}{\partial t} = \frac{\partial^2 N_\kappa}{\partial X^2}, \tag{14}$$

in the domain: $D_n = \left\{ t > 0, X \in (0,1), Z \in \bigcup_{k=1}^{n+1} (L_{k-1}, L_k); L_0 = 0; L_{n+1} \equiv 1 \right\}$

with the initial conditions:

$$C_k(t=0,Z) = 0; \quad N_k(t=0,X,Z) = 0; \tag{15}$$

the boundary conditions:

$$C_{n+1}\left(t, Z=1\right)=1; \qquad N_k\left(t, X=1, Z\right)=C_k\left(t, Z\right); \tag{16}$$

$$\frac{\partial C_1}{\partial Z}(t, Z=0)=0, \qquad N_k\left(t, X=0, Z\right)=0 \tag{17}$$

and the interface conditions:

$$\left[C_k\left(t,Z\right)-C_{k+1}\left(t,Z\right)\right]_{Z=L_k}=0;\left[\frac{\partial}{\partial Z}C_k\left(t,Z\right)-\frac{\partial}{\partial Z}C_{k+1}\left(t,Z\right)\right]_{Z=L_k}=0; k=\overline{1,n} \tag{18}$$

Analytical solution: concentration profiles

The analytical solutions of the problem described by Eqs. (13)-(18) can be obtained using the Laplace integral transformation and the Cauchy function methods developed in appendix. They give the concentration profiles of the diffusant in each layer of the bed: $C_k(t,Z)$ in the macropores and $Q_k(t,X,Z)$ in the crystallites (micropores) situated in the bed at a height Z.

For reasons of homogeneity the numbers of the following equations correspond to those of the equations obtained after the development in appendix I.

$$C_k(t,Z)=1+\sum_{j=1}^{\infty}\frac{exp\left(-\beta_j^2\cdot t\right)}{\beta_j^2\cdot d\delta\left(\beta_j\right)}\begin{cases}\prod\limits_{j=1}^{n}\varphi_{j+1}(\beta)\cdot cos\left[\varphi_1(\beta)Z\right] & ;k=1\\ \prod\limits_{j=k}^{n}\varphi_{j+1}(\beta)\cdot\left[\Phi_{22}^{k-1}(\varphi_k(\beta)L_{k-1},\varphi_k(\beta)Z)\cdot\delta_{\overline{1,2k-1}}(\beta)-\Phi_{12}^{k-1}(\varphi_k(\beta)L_{k-1},\varphi_k(\beta)Z)\cdot\delta'_{\overline{1,2k-1}}(\beta)\right] & ;k=\overline{1,n};\\ \left[\Phi_{22}^{n}(\varphi_{n+1}(\beta)Z,\varphi_{n+1}(\beta)L_{n+1})\cdot\delta_{\overline{1,2n-1}}(\beta)-\Phi_{12}^{n}(\varphi_{n+1}(\beta)Z,\varphi_{n+1}(\beta)L_{n+1})\cdot\delta'_{\overline{1,2n-1}}(\beta)\right] & ;k=n+1\end{cases} \tag{46}$$

$$Q_k(t,X,Z)=\frac{2\pi}{\tau_{m_k}}\sum_{j_1=0}^{\infty}j_1(-1)^{j_1+1}\frac{sin(j_1\pi\cdot X)}{X\cdot\mu_{j_1}^2}\cdot$$

$$\cdot\left(1-exp\left(-\mu_{j_1}^2\cdot t\right)\cdot\left[1-\sum_{j=1}^{\infty}\frac{\varepsilon_{j_1j}(t)}{\beta_j^2\cdot d\delta\left(\beta_j\right)}\begin{cases}\prod\limits_{j=1}^{n}\varphi_{j+1}(\beta)\cdot cos\left[\varphi_1(\beta)Z\right] & ;k=1\\ \prod\limits_{j=k}^{n}\varphi_{j+1}(\beta)\begin{bmatrix}\Phi_{22}^{k-1}(\varphi_k(\beta)L_{k-1},\varphi_k(\beta)Z)\cdot\delta_{\overline{1,2k-1}}(\beta)-\\ -\Phi_{12}^{k-1}(\varphi_k(\beta)L_{k-1},\varphi_k(\beta)Z)\cdot\delta'_{\overline{1,2k-1}}(\beta)\end{bmatrix} & ;k=\overline{1,n}\\ \begin{bmatrix}\Phi_{22}^{n}(\varphi_{n+1}(\beta)Z,\varphi_{n+1}(\beta)L_{n+1})\cdot\delta_{\overline{1,2n-1}}(\beta)-\\ -\Phi_{12}^{n}(\varphi_{n+1}(\beta)Z,\varphi_{n+1}(\beta)L_{n+1})\cdot\delta'_{\overline{1,2n-1}}(\beta)\end{bmatrix} & ;k=n+1\end{cases}\right]\right); \tag{50}$$

where

$$\varepsilon_{j_1j}(t)=\begin{cases}1-exp\left[-(\beta_j^2-\mu_{j_1}^2)t\right] & ;j_1\neq j\\ t & ;j_1=j\end{cases}. \tag{51}$$

Here: $\beta_j; j=\overline{1,\infty}$ are the roots of transcendental equation:

$$\delta(\beta)=\delta_{12}(\varphi_{n+1}(\beta)L_n,\varphi_{n+1}(\beta)L_{n+1})\cdot\delta'_{\overline{1,2n-1}}(\beta)-\delta_{22}(\varphi_{n+1}(\beta)L_n,\varphi_{n+1}(\beta)\cdot\delta_{\overline{1,2n-1}}(\beta); \tag{42}$$

This equation corresponds to the expression of the determinant $\Delta^*(s)\big|_{s=-\beta^2}$ of the Laplace system [Eqs. (41) and (42) in appendix I].

$d\delta(\beta)$: analytical expression for the calculation of the derivative of the determinant $\Delta^*(s)\big|_{s=-\beta^2}$ (according to Heavyside's theorem);

$$\varphi_k(\beta) = -\gamma_k(s)\big|_{s=\beta^2} = \sqrt{\Gamma_k\left(\frac{P_{\text{inter},k}}{3}\tau_{m,k}\beta^2 + \left[1 - \sqrt{\tau_{m,k}}\beta \cdot ctg\left(\sqrt{\tau_{m,k}}\beta\right)\right]\right)};$$

corresponds to Eq. (43) of appendix I.

$\delta_{mj}(\varphi_k(\beta)L_{k-1}, \varphi_k(\beta)L_k) = -i \cdot \Delta_{mj}(\gamma_k(s)L_{k-1}, \gamma_k(s)L_k); m, j = \overline{1,2}$ - ;

$\delta_{\overline{1,2k-1}}(\beta) = -i^{k-1} \cdot \Delta_{\overline{1,2k-1}}(s)\big|_{s=-\beta^2}; \delta'_{\overline{1,2k-1}}(\beta) = -i^{k-1} \cdot \Delta'_{\overline{1,2k-1}}(s)\big|_{s=-\beta^2}$: recurrent structures which are used in the calculation of the determinant $\Delta^*(s)\big|_{s=-\beta^2}$;

$\Phi^k_{mj}(\varphi_k(\beta)L_{k-1}, \varphi_k(\beta)Z); m, j = \overline{1,2}$: recurrent functions which are combinations of $\cos(\varphi(\beta)L_k)$ $\sin(\varphi(\beta)L_k)$ (appendix I)

Experimental Results: Benzene adsorption curves

Fig. 4 represents the variation with time of the benzene concentration for each level of the zeolite bed. It must be noted that the z coordinate is determined relative to the bottom of the tube. For example, z = 15 mm (dimensionless Z = 1) corresponds to the surface of the bed directly in contact with the gas phase.

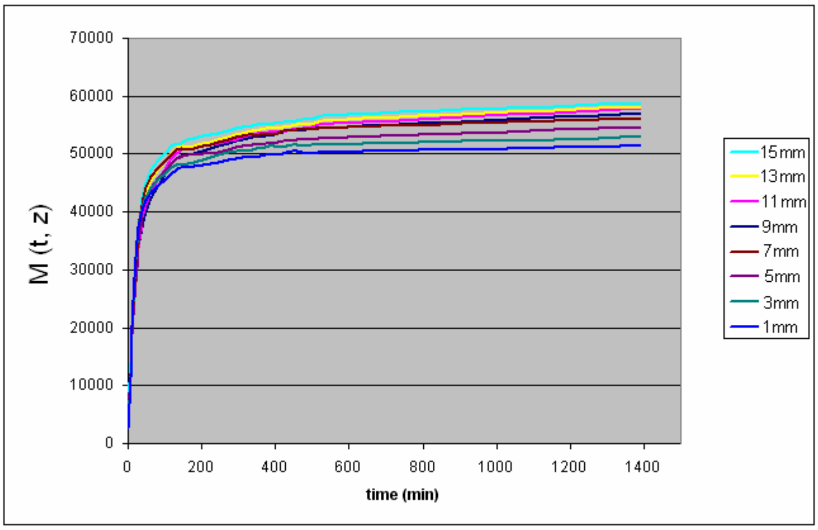

Fig. 4. Amount (arbitrary units) of adsorbed benzene against time in each layer *k* of the bed, from z = 15 mm (layer in contact with the gas phase) to z = 1 mm (layer near the bottom of the bed).

The amount of adsorbed benzene at the equilibrium of adsorption is 1.25 mmol.g^{-1}, in agreement with reference [23].

Numerical simulation and analysis

Modeling procedure

A program in the Microsoft Visual C++ environment was especially developed to provide solutions to the following problems:

1) *Inverse problem*. Experimental data relative to benzene adsorption kinetics in the zeolite bed are collected. An analytical solution is applied to these data. Based on these data and the analytical solution, the diffusion coefficient profiles in the macropores (intercrystallite space) D_{inter} and in the micropores of the crystallites (intracrystallite space) D_{intra} are found by the program. This allows us to develop a procedure to check the adequacy of the model and also allows further modeling of concentration profiles and other parameters.
2) *Direct problem*. Using the diffusion coefficient profiles D_{inter} and D_{intra}, the program can determine the concentration distribution in the intercrystallite space $C(t,Z)$, in the intracrystallite space $Q(t,X,Z)$ and the integral mass $M(t,Z)$.

Solution of the inverse problem: Calculation of the diffusion coefficients D_{inter} **and** D_{intra}

Using the experimental curves of Fig. 4 and modeling absorbent concentration profiles in macropores, C, in micropores, Q, according to Eqs. (46) and (50), we compute the diffusion coefficients profiles D_{inter} and D_{intra}.

Fig. 5 shows the computed variations of D_{inter} and D_{intra} versus time at four different distances z (in mm) from the bottom of the bed: z = 14; z = 10; z = 7; z = 3. As we can see, D_{inter} and D_{intra} decrease approximately exponentially with time increase, which is normal since the crowding increases in parallel with the concentration of adsorbed molecules. D_{inter} decreases from 1.4 m^2/s at the beginning of adsorption to 0.001 m^2/s near the equilibrium state. In the same way, D_{intra} decreases from 10^{-12} to $5{\cdot}10^{-14}$ m^2/s. These results are in good agreement with the literature data [24, 25].

It may appear surprising that the beginning of the curve corresponding to z = 14 mm presents a lower diffusion coefficient than the others for the same time. This is due to the fact that there is not a perfect concordance between the moment the solid comes into contact with the benzene and the acquisition of the first NMR signals. The first signals correspond then to the upper layers which have already adsorbed a significant amount of gas, making thus diffusion more difficult.

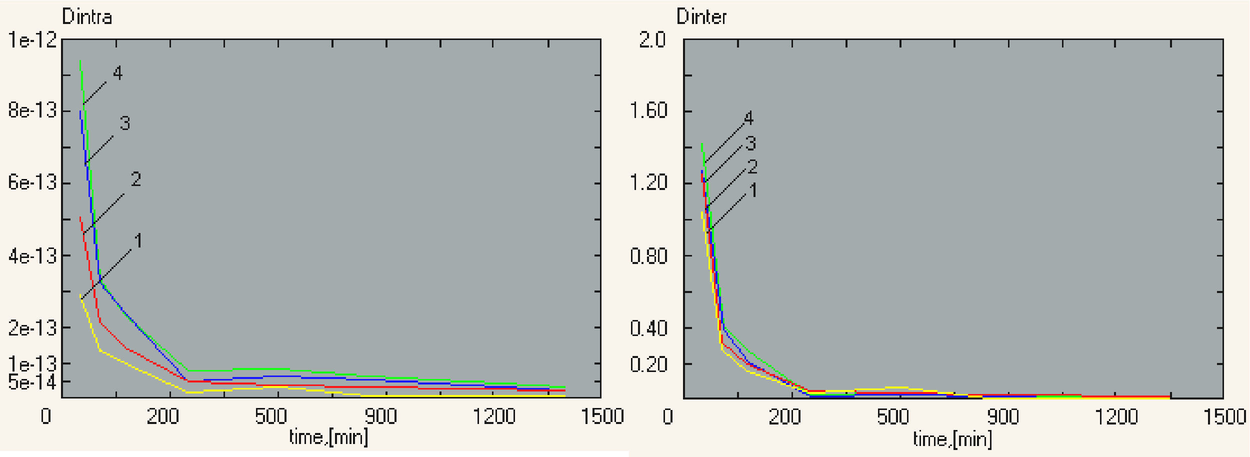

Figure 5. Benzene diffusion coefficient profiles D_{intra} and D_{inter} (m^2/s) against time t (min)
Curves: 1) z = 14 mm; 2) z = 10 mm; 3) z = 7 mm; 4) z = 3 mm.

Solution of the direct problem: Using the values of D_{inter} and D_{intra} (Fig. 5) we can determine the concentration distributions in the intercrystallite space $C(t,z)$ (Eq. 46), in the intracrystallite space $Q(t,X,z)$ (Eq. 50) and the total adsorbed mass $M(t,z)$, for each time and position in the bed (z) and in the crystallites (z,r).

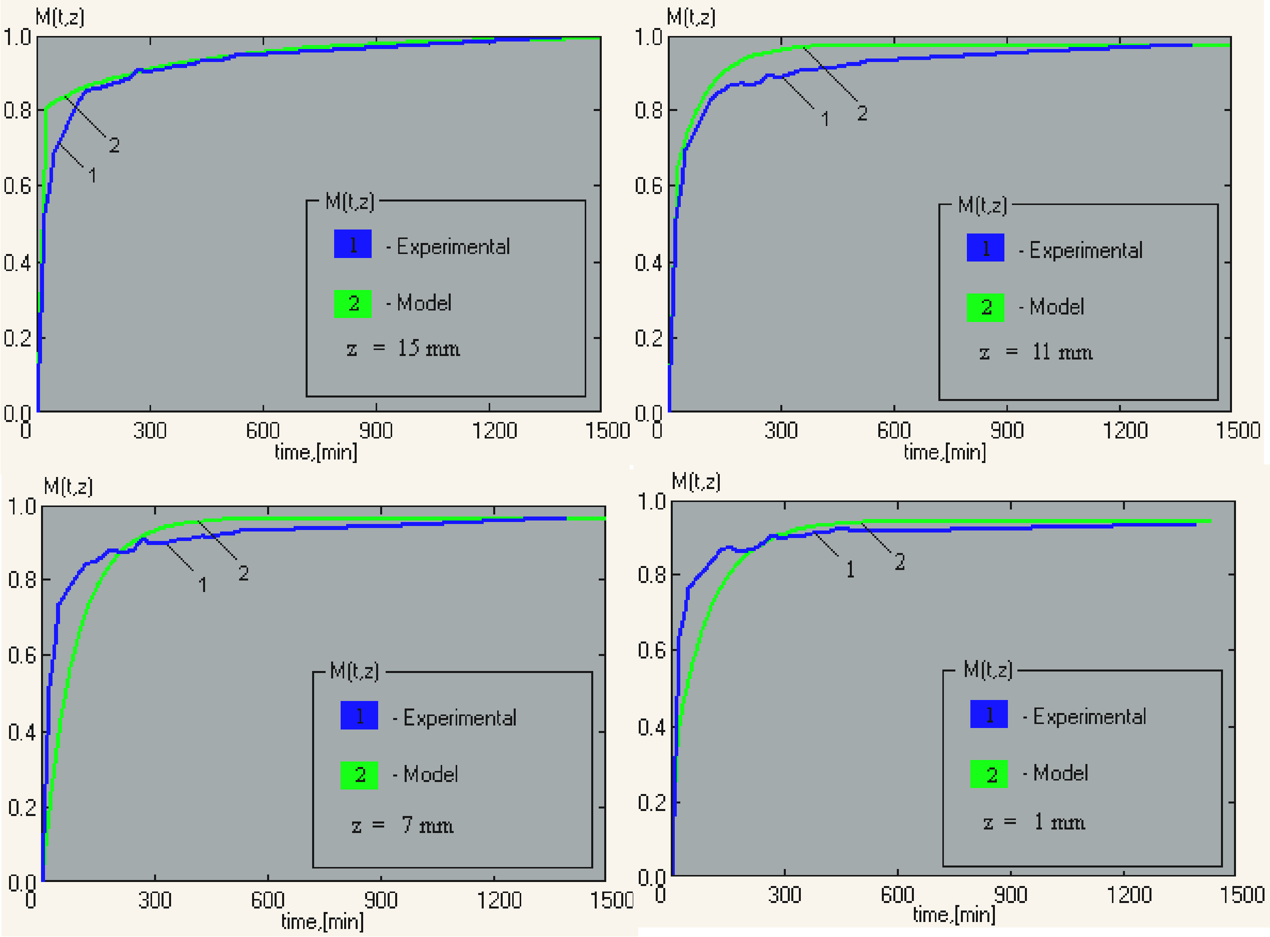

Fig.6. Model and experimental kinetic curves of dimensionless total adsorbed mass versus time t (min) for different values of distance (mm) from the bottom of the zeolite bed z.

For example, Fig.6 shows the calculated and experimental kinetic curves of dimensionless total adsorbed mass $M(t,z)$ versus time t for four positions z (mm) from the bottom of the bed: *z = 15 mm; z = 11 mm; z = 7 mm; z = 1 mm*. The calculated variations agree satisfactorily with the experimental ones.

Fig.7 shows the concentration profiles of C_6H_6 in intercrystalline space C(t,z) for four positions z. Near the top of the bed, *z=15-13* mm ($Z \approx 1$), the concentration profiles C(t,z) are approaching to 1 according to the dimensionless boundary condition (10). This convergence is also theoretically ensured by the methods used to determine the analytical solution of the model (7)-(12) [26-28].

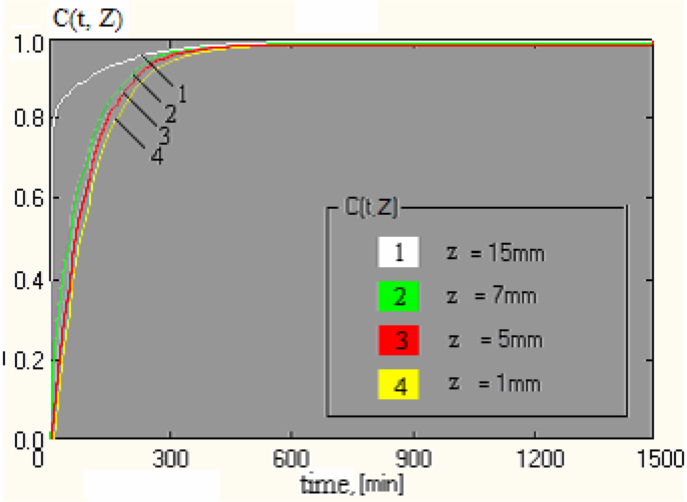

Figure 7. Intercrystallite concentration profiles versus time t (min) for different values of the distance z (mm) from the bottom of the bed

Fig. 8 presents the calculated profiles of C_6H_6 concentrations in crystallites, $Q(t,X,z)$, as a function of dimensionless distance from the crystallite center X for different times *t* (min) and four distances from the bottom of the crystallite bed z (*mm*). The concentration gradient $Q(t,X,z)$ depends of course on the adsorption time but also, very much, on the position of the crystallites in the bed as well as on the abscissa of these latter. This gradient is always greater near the surface of the crystallites, r =R (X = 1), than at the center, r =0 (X = 0). In the same way, the gradient increases with the depth in the bed. For instance, at distances z = 1, 5 and 7 *mm* the maximum of the concentration gradient is 0.21, 0.13 and 0.12 (we remind that Q and X are dimensionless). Near the top of the bed, z = 15 *mm*, the concentration gradient is roughly negligible whatever t.

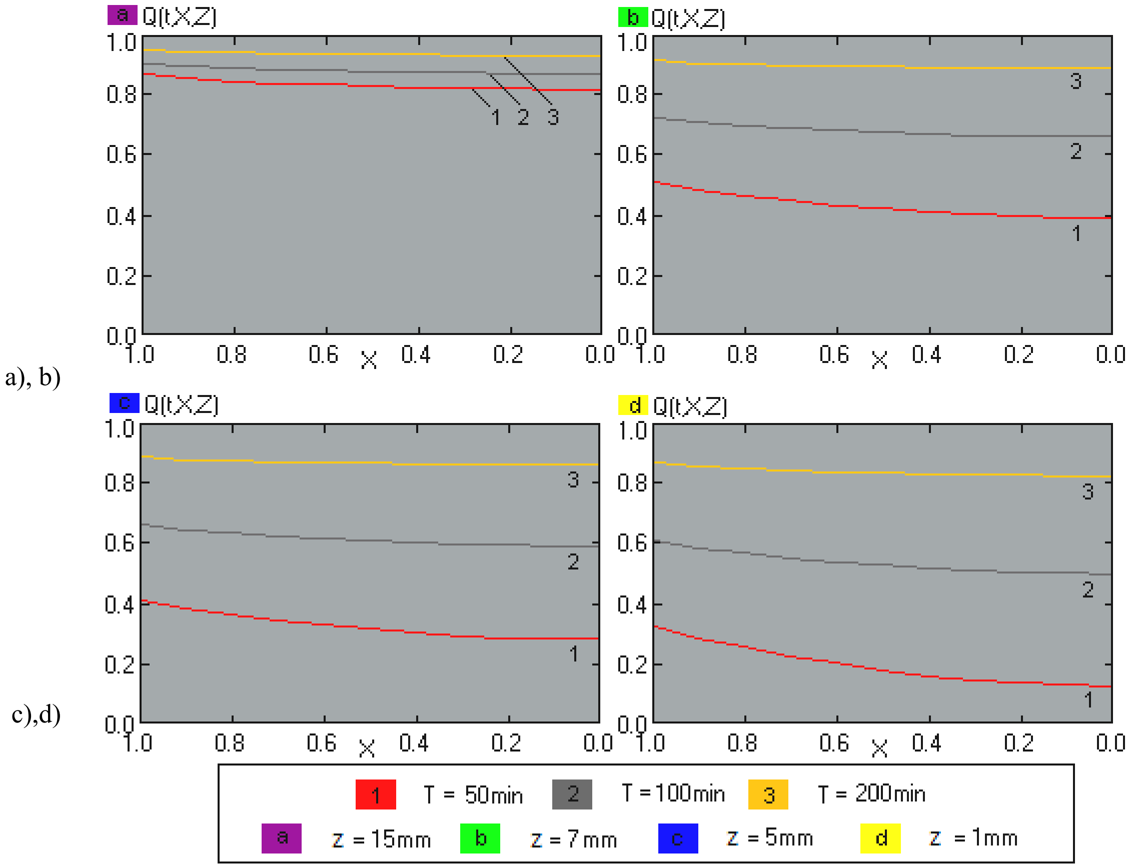

Fig. 8. Concentration profiles, *Q(t,X,z)*, in zeolite crystallites located at different positions *z* (*mm*) in the bed, and for different times t (min.): a) *z = 15 mm*; b) *z = 7 mm*; c) *z = 5 mm*; d) *z = 1 mm*.

Conclusion

We have presented the analytical solution of the equations of gas diffusion in a zeolite bed, assuming it to consist of a large number of very thin layers of solid, perpendicular to the direction of propagation of the gas. The solution is based on the integral Laplace transformation and Cauchy methods. We have applied the analytical solution to the study of benzene diffusion in the macropores and micropores of a ZSM5 zeolite bed.

The solution of the inverse problem makes possible the calculation, from experimental data, of the inter- and intracrystallite diffusion coefficients, D_{inter} and D_{intra}, respectively, as a function of time and the crystallite position in the bed.

The solution of the direct problem allows the estimation of the concentration profiles, concentration gradient profiles and other parameters inside the micro- and macropores of a ZSM5 bed. There is good agreement between experimental and model kinetic curves for the thin layers at different positions of the bed.

This technique should prove to be very interesting for studying the co-diffusion of several gases in a catalytic bed, since it should make it possible to detect the characteristic spectra of each gas at every moment and position in the bed.

Nomenclature

$k = \overline{1, n+1}$: layer number. Subscript *k* will be added to all the following symbols to specify that they are characteristic of the *k* layer.

c : adsorbate concentration in macropores.

c_∞ : adsorbate equilibrium concentration in macropores.

$C = c/c_\infty$: dimensionless adsorbate concentration in macropores.

D_{inter} : macropore diffusion coefficient, m^2/s

D_{intra} : micropore diffusion coefficient, m^2/s

K : adsorption equilibrium constant

l : bed length, mm.

$\Delta l = l_k - l_{k-1}; k = \overline{1, n+1}$: layer thickness (we assume that all layers have the same thickness)

L: dimensionless bed length

M_m : micropore uptake.

M_M : macropore uptake.

M_t : total uptake at time t.

M_∞ : total uptake at equilibrium.

p_{inter} : relative adsorbed gas in macropores in equilibrium condition.

p_{intra} : relative adsorbed gas in micropores in equilibrium condition.

q : adsorbate concentration in micro- and nanopores.

q_∞ : equilibrium adsorbate concentration in micropores.

$Q = q/q_\infty$: dimensionless adsorbate concentration in nanopores.

r : distance from crystallite center, mm.

R : mean crystallite radius, mm (we assume that the crystallites are spherical).

$X = r/R$: dimensionless distance from crystallite center.

z : distance from bottom of crystallite bed, mm.

$Z = z/l$: dimensionless distance from bottom of the crystallite bed.

Greek letters

ε_{inter} : bed porosity.

τ_M : diffusion time required for a molecule to penetrate the crystallite bed from top to bottom, s.

τ_m : diffusion time required for a molecule to penetrate a crystallite from the external surface to the center, s.

τ_{inter} : time constant of diffusion in intercrystallite space, s .

τ_{intra} : time constant of diffusion in intracrystallite space, s .

Γ : dynamic parameter.

References

1- Lykov A.V. and Mykhaylov Y.A., *The Theory of Mass Transport,* State Energy Publishing, Moscow (1963).

2- Ruckenstein E., Vaidyanathan A.S. and Youngquist G.R., *Sorption by Solids with Bidisperse Pore Structures,* Chem. Eng. Sci., **26**, 147-152 (1971).

3- Barrer R.M*., Diffusion and Flow in Porous Zeolite, Carbon or Ceramic Media, Characterization of Porous Solids*, Society of Chemical Industry, London (1979).

4- Kärger J. and Ruthven D., *Diffusion in Zeolites and Other Microporous Solids*, John Wiley & Sons, New York (1992) and references therein.

5- Chen N.Y., Degnan T.F. and Smith M.C., *Molecular Transport and Reaction in Zeolites: Design and Application of Shape Selective Catalysis*, VCH, Weinheim and New York (1994).

6- Lee L.K., *The kinetics of sorption in a biporous adsorbent particle*, AIChE J*.,* **24**, 531-533 (1978).

7- Magalhães F.D., Laurence R.L., Conner, W.C., Springuel-Huet M.A., Nosov A. and Fraissard J., *Study of molecular transport in beds of zeolite crystallites: semi-quantitative modeling of* ^{129}*Xe NMR experiments,* J. Phys. Chem. B, **101**, 2277-2284 (1997).

8- Springuel-Huet M.A., Nosov A., Kärger J. and Fraissard J., ^{129}*Xe NMR study of bed resistance to molecular transport in assemblages of zeolite crystallites*, J. Phys. Chem., **100**, 7200-7203 (1996).

9- N'Gokoli-Kekele P., Springuel-Huet M.A. and Fraissard J., *An Analytical Study of Molecular Transport in a Zeolite Crystallite Bed.* Adsorption, **8**, 35-44 (2002)

10- Petryk M., Shabliy O., Leniyk M. and Vasylyuk P., *Mathematical Modeling and Research for Diffusion Process in Multilayer and Nanoporous Media.* Fluid Transport in Nanoporous Materials. (W.C. Conner and J. Fraissard, eds.), NATO Science Series, Series II: Mathematics, Physics and Chemistry, Vol. 219. Springer (Amsterdam) 685-655 (2006).

11 - Kärger, J., *A study of fast tracer desorption in molecular sieve crystals,* AIChE J., **28**, 417-423 (1982).

12- Kärger, J. and Heink W., *The propagator representation of molecular transport in microporous crystallites*, J. Magn. Reson., **51**, 1 (1983).

13- Kärger J. and Pfeifer H., *NMR self-diffusion studies in zeolite science and technology*, Zeolites, **7**, 90-107 (1987).

14- Kärger J., Pfeifer H. and Heink W., *Advances in Magnetic Resonance*. (J.S. Waugh, ed.), Vol. **12**, p. 1, Academic Press, San Diego, 1988.

15- Koresh, J. and Soffer, A.J., *Molecular Sieve Carbons, Part 3 – Adsorption kinetics according to a surface barrier model*, Chem. Soc. Faraday Trans., **77**, 3005-3018 (1981).

16- Ma, Y.H. and Ho S.Y., *Diffusion in synthetic fine powder and pellets,* AIChE J.*,* **20**, 279-283 (1974).

17- Ma, Y.H. and Lee T.Y., *Transient diffusion in solids with a bipore distribution*, AIChE J., **22**, 147-152 (1976).

18- Ruthven, D.M., *Principles of Adsorption and Adsorption Processes*, Wiley, New York, 1984.

19- Younquist, G.R., *Diffusion and flow of gases in porous solids*, Ind. Eng. Chem., **62**, 52-63 (1970).

20- Leclerc S., Trausch G., Cordier B., Grandclaude D., Retournard A., Fraissard J. and Canet D., *Chemical Shift Imaging (CSI) by precise Object Displacement,* Magn. Reson. Chem., **44,** 311-317 (2006).

21- Petryk M. and Vorobiev E., *Mass Transfer from Liquid containing Spherical Particles During The Pressing of Biological Porous Material*, Proceedings of the 2nd W. European Conference on Filtration and Separation, Compiègne (France), Vol. 2, 763-766 (2000).

22- Petryk M., Petryk N and Matiega V., *The Intensification of Process of Vibrofiltration in non Regular Cylindrical Media.* Emerging Solid/Liquid Separation Technologies ICEST-2002, Compiègne (France), **1,** 143-149 (2002).

23- Foger K. , Sanders J.V. and Seddon D., *Channel arrangements and activity of some ZSM zeolites.* Zeolite, **4,** 337-345 (1984).

24- Springuel-Huet M.-A., *^{129}Xe NMR for diffusion of hydrocarbons in zeolites and ^{1}H NMR imaging for competitive diffusion of binary mixtures of hydrocarbons in zeolites*
Fluid Transport in Nanoporous Materials (2006)
NATO Science series II ¨Mathematics, Physics and Chemistry, Vol.219, pp 315- 332.
Wm. Curtis Conner and Jacques Fraissard, Edit., Springer , Dordrecht, Publisher.

25- Jobic H., *Diffusion in zeolites measured by neutron scattering techniques*
Fluid Transport in Nanoporous Materials (2006)
NATO Science series II ¨Mathematics, Physics and Chemistry, Vol.219, pp 333-352.
Wm. Curtis Conner and Jacques Fraissard, Edit., Springer , Dordrecht, Publisher.

26- Leniuk M.P. and Petryk M.R. *The method of integral transformations of Fourier- Bessel with spectral parameter in mathematical modeling of the mass exchange process in no regular media,* Kiev, (UA), Naukova Dumka (Academic Publishing), 372 (2000).

27- Petryk M.R., *The mathematical modeling of adsorption and diffusion process in the liquid or gas flow. The integral transformation and their application for boundary problems.* Academy National Institute Mathematical Bulletin, **3**, 220-233 (1993).

28- Leniuk M.P. and Petryk M.R., *The mathematical modeling of mass transfer in heterogeneous multi-interface microporous medias. Ternopil State Technical University Bulletin,* (Ukraine), **4,** 147-158 (2004)

29- Lavrentiev M.A. and Shabat B.V., *The complex variable theory methods.* Science, Moscow, 1965.

Appendix I

Analytical solution

Applying the integral Laplace transformation to Eq. (13–18), one obtains Eq. (22)-(29) [29]:

$$\frac{d^2C_k^*(s,Z)}{dZ^2} = \tau_{M,k} \cdot s \cdot C_k^* + \Gamma_k \cdot \left[\frac{\partial N_k^*}{\partial X} - N_k^* \right]_{X=1}^{(s,X,Z)}; \tag{22}$$

$$\frac{d^2N_k^*(s,X,Z)}{dX^2} = \tau_{m,k} \cdot s \cdot N_k^* \tag{23}$$

in the domain: $D_n^* = \left\{ X \in (0,1), Z \in \bigcup_{k=1}^{n+1} (L_{k-1}, L_k); L_0 = 0; L_{n+1} \equiv 1 \right\}$

with the boundary conditions:

$$C_{n+1}^*(s,Z=1) = \frac{1}{s}; \frac{\partial C_1^*(s,Z=0)}{\partial Z} = 0; \tag{24}$$

$$N_k^*(s,X=1,Z) = C_k^*(s,Z); \qquad N_k^*(s,X=0,Z) = 0; \tag{25}$$

and the interfaces conditions:

$$\left[C_k^*(s,Z) - C_{k+1}(s,Z) \right]_{Z=L_k} = 0; \left[\frac{\partial}{\partial Z} C_k^*(s,Z) - \frac{\partial}{\partial Z} C_{k+1}^*(s,Z) \right]_{Z=L_k} = 0; k = \overline{1,n}, \tag{26}$$

here $C_k^*(s,Z) \equiv \tilde{\mathcal{L}}\left[C_k(t,Z) \right] = \int_0^\infty C_k(t,Z) \cdot exp(-st)dt;$

$N_k^*(s,X,Z) \equiv \tilde{\mathcal{L}}\left[N_k(t,X,Z) \right] = \int_0^\infty N_k(t,X,Z) \cdot exp(-st)dt,$

$s = \sigma + i\omega$ is a complex variable of the Laplace transformation.

The general solution of Eq. (23) is of the form:

$$N_k^*(s,X,Z) = a_k(s,Z)\cdot ch\left[\sqrt{\tau_{m,k}s}X\right] + b_k(s,Z)\cdot sh\left[\sqrt{\tau_{m,k}s}X\right]. \tag{27}$$

Substituting Eq. (27) into conditions (25) one obtains:

$$N_k^*(s,X,Z) = C_k^*(s,Z)\cdot\frac{sh\left[\sqrt{\tau_{m,k}s}X\right]}{sh\left[\sqrt{\tau_{m,k}s}\right]} \tag{28}$$

Determining the expressions:

$$N_k^*(s,1,Z) = C_k^*(s,Z);\qquad \left.\frac{\partial N_k^*(s,X,Z)}{\partial X}\right|_{X=1} = \tau_{m,k}s\cdot C_k^*(s,Z)\cdot cth\left[\sqrt{\tau_{m,k}s}\right]$$

and substituting them into Eq. (22), the latter will become as follows:

$$\frac{d^2C_k^*(s,Z)}{dZ^2} = \gamma_k^2(s)\cdot C_k^*(s,Z); \tag{29}$$

with:

$$\gamma_k^2(s) = \tau_{M,k}s + \Gamma_k\left(\sqrt{\tau_{m,k}s}\cdot cth\sqrt{\tau_{m,k}s} - 1\right) \equiv \Gamma_k\left(\frac{p_{\mathrm{inter},k}}{3}\tau_{m,k}s + \sqrt{\tau_{m,k}s}\cdot cth\sqrt{\tau_{m,k}s} - 1\right);$$

$$k = \overline{1,n+1}. \tag{30}$$

The general solution of Eq. (29) with the boundary conditions (24) and interface conditions (26) is [26-28]:

$$C_1^*(s,Z) = A_1(s)\cdot ch\left[\gamma_1(s)Z\right]; \tag{31}$$

$$C_k^*(s,Z) = A_k(s)\cdot ch\left[\gamma_k(s)Z\right] + B_k(s)\cdot sh\left[\gamma_k(s)Z\right]; k = \overline{2,n+1}. \tag{32}$$

where A_1, A_k, B_k are unknown constants to be found. $k = \overline{2,n+1}$.

Symbolizing:

$$V_{11}^{01}(\gamma_1(s)\cdot 0) = \gamma_1 sh(\gamma_1\cdot 0) = 0; V_{11}^{02}(\gamma_1(s)\cdot 0) = \gamma_1 ch(\gamma_1\cdot 0) = \gamma_1; \tag{33}$$

$$V_{1j}^{k1}(\gamma_m(s)\cdot L_k) = ch(\gamma_m L_k); V_{1j}^{k2}(\gamma_m(s)\cdot L_k) = sh(\gamma_m L_k);$$

$$V_{2j}^{k1}(\gamma_m(s)L_k) = \gamma_m(s)\cdot sh(\gamma_m L_k); V_{2j}^{k2}(\gamma_m(s)\cdot L_k) = \gamma_m(s)\cdot ch(\gamma_m L_k); \tag{34}$$

$$V_{22}^{n+1,1}(\gamma_{n+1}(s)L_{n+1}) = ch(\gamma_{n+1}(s)L_{n+1}); V_{22}^{n+1,2}(\gamma_{n+1}(s)L_{n+1}) = sh(\gamma_{n+1}(s)L_{n+1}); \tag{35}$$

$$\Phi_{ij}^{k}(\gamma_m L_k,\gamma_m Z)=V_{ij}^{k2}(\gamma_m L_k)ch\gamma_S Z-V_{ij}^{k1}(\gamma_m L_k)sh\gamma_m Z;i,j=\overline{1,2};m=\begin{cases}k & ;j=1\\ k+1 & ;j=2\end{cases}.$$

Using the boundary (24) and the interface (26) conditions one obtains the algebraic equation system:

$$\begin{cases}
V_{11}^{11}\left(\gamma_1 L_1\right)\cdot A_1-V_{12}^{11}\left(\gamma_2 L_1\right)\cdot A_2-V_{12}^{12}\left(\gamma_2 L_1\right)\cdot B_2=0\\
V_{21}^{11}\left(\gamma_1 L_1\right)\cdot A_1-V_{22}^{11}\left(\gamma_2 L_1\right)\cdot A_2-V_{22}^{12}\left(\gamma_2 L_1\right)\cdot B_2=0\\
V_{11}^{21}\left(\gamma_2 L_2\right)A_2+V_{11}^{22}\left(\gamma_2 L_2\right)B_2-V_{12}^{21}\left(\gamma_3 L_2\right)A_3-V_{12}^{22}\left(\gamma_3 L_2\right)B_3=0\\
V_{21}^{21}\left(\gamma_2 L_2\right)A_2+V_{21}^{22}\left(\gamma_2 L_2\right)B_2-V_{22}^{21}\left(\gamma_3 L_2\right)A_3-V_{22}^{22}\left(q_3 L_2\right)B_3=0\\
-------------------------------\\
V_{11}^{k1}\left(\gamma_k L_k\right)A_k+V_{11}^{k2}\left(\gamma_k L_k\right)B_k-V_{12}^{k1}\left(\gamma_{k+1} L_k\right)A_{k+1}-V_{12}^{k2}\left(\gamma_{k+1} L_k\right)B_{k+1}=0\\
V_{21}^{k1}\left(\gamma_k L_k\right)A_k+V_{21}^{k2}\left(\gamma_k L_k\right)B_k-V_{22}^{k1}\left(\gamma_{k+1} L_k\right)A_{k+1}-V_{22}^{k2}\left(\gamma_{k+1} L_k\right)B_{k+1}=0\\
V_{11}^{k+1,1}\left(\gamma_{k+1} L_{k+1}\right)A_{k+1}+V_{11}^{k+1,2}\left(\gamma_{k+1} L_{k+1}\right)B_{k+1}-V_{12}^{k+1,1}\left(\gamma_{k+2} L_{k+1}\right)A_{k+2}-V_{12}^{k+1,2}\left(\gamma_{k+2} L_{k+1}\right)B_{k+2}=0\\
V_{21}^{k+1,1}\left(\gamma_{k+1} L_{k+1}\right)A_{k+1}+V_{21}^{k+1,2}\left(\gamma_{k+1} L_{k+1}\right)B_{k+1}-V_{22}^{k+1,1}\left(\gamma_{k+2} L_{k+1}\right)A_{k+2}-V_{22}^{k+1,2}\left(\gamma_{k+2} L_{k+1}\right)B_{k+2}=0\\
-------------------------------\\
V_{11}^{n,1}\left(\gamma_n L_n\right)A_n+V_{11}^{n,2}\left(\gamma_n L_n\right)B_n-V_{12}^{n,1}\left(\gamma_{n+1} L_n\right)A_{n+1}-V_{12}^{n,2}\left(\gamma_{n+1} L_n\right)B_{n+1}=0\\
V_{21}^{n,1}\left(\gamma_n L_n\right)A_n+V_{21}^{n,2}\left(\gamma_n L_n\right)B_n-V_{12}^{n,1}\left(\gamma_{n+1} L_n\right)A_{n+1}-V_{22}^{n,2}\left(\gamma_{n+1} L_n\right)B_{n+1}=0\\
V_{22}^{n+1,1}\left(\gamma_{n+1} L_{n+1}\right)A_{n+1}+V_{22}^{n+1,2}\left(\gamma_{n+1} L_{n+1}\right)B_{n+1}=1/s
\end{cases}. \tag{36}$$

Assuming that the determinant of the coefficients of system (36), $\Delta^*(s)\neq 0$, we write the solution in the form:

$$C_k^*(s,Z)=\frac{1}{s\cdot\Delta^*(s)}\begin{cases}\prod\limits_{j=1}^{n}\gamma_{j+1}\cdot ch\left[\gamma_1(s)Z\right] & ;k=1\\ \prod\limits_{j=k}^{n}q_{j+1}\left[\mathit{\Phi}_{22}^{k-1}(\gamma_k L_{k-1},\gamma_k Z)\cdot\Delta_{\overline{1,2k-1}}-\mathit{\Phi}_{12}^{k-1}(\gamma_k L_{k-1},\gamma_k Z)\cdot\Delta'_{\overline{1,2k-1}}\right] & ;k=\overline{1,n}\\ \left[\mathit{\Phi}_{22}^{n}(\gamma_{n+1}Z,\gamma_{n+1}L_{n+1})\cdot\Delta_{\overline{1,2n-1}}-\mathit{\Phi}_{12}^{n}(\gamma_{n+1}Z,\gamma_{n+1}L_{n+1})\cdot\Delta'_{\overline{1,2n-1}}\right] & ;k=n+1\end{cases}; \tag{37}$$

$$N_k^*(s,X,Z)=C_k^*(s,Z)\cdot\frac{sh\left[\sqrt{\tau_{m,_k}s}X\right]}{sh\left[\sqrt{\tau_{m,_k}s}\right]}=\frac{1}{s}W_{l,_k}^*(s,Z)\cdot\frac{sh\left[\sqrt{\tau_{m,_k}s}X\right]}{sh\left[\sqrt{\tau_{m,_k}s}\right]}\equiv C_k^*(s,Z)\cdot\omega_k^*(s,X); \tag{38}$$

here:

$$W^*_{l,_k}(s,Z)=\frac{1}{\Delta^*(s)}\begin{cases}\prod\limits_{j=1}^{n}\gamma_{j+1}\cdot ch\left[\gamma_1(s)Z\right] & ;k=1\\ \prod\limits_{j=k}^{n}q_{j+1}\left[\varPhi_{22}^{k-1}(\gamma_k L_{k-1},\gamma_k Z)\cdot\Delta_{\overline{1,2k-1}}-\varPhi_{12}^{k-1}(\gamma_k L_{k-1},\gamma_k Z)\cdot\Delta'_{\overline{1,2k-1}}\right] & ;k=\overline{1,n}\\ \left[\varPhi_{22}^{n}(\gamma_{n+1}Z,\gamma_{n+1}L_{n+1})\cdot\Delta_{\overline{1,2n-1}}-\varPhi_{12}^{n}(\gamma_{n+1}Z,\gamma_{n+1}L_{n+1})\cdot\Delta'_{\overline{1,2n-1}}\right] & ;k=n+1\end{cases}\quad. \tag{39}$$

The calculations of determinants $\Delta^*(s)$ of the coefficients of system (36) and determinants $\Delta_{\overline{1,2k-1}}$ and $\Delta'_{\overline{1,2k-1}}$ are shown in appendix II.

Return to the original function. According to Vasthenco-Zaharthenco's theorem [1] and Heavyside's theorem [2] the original function of a Laplace transform function is:

$$F(t)=\int\limits_0^{\infty}\frac{f(s)}{s\cdot g(s)}exp(st)\,dt=\frac{f(s=0)}{g(s=0)}+\sum_{j=1}^{\infty}\frac{f(s)}{s_j\cdot\left.\dfrac{dg(s)}{ds}\right|_{s=s_j}}exp(s_jt), \tag{40}$$

where s_j are the different positive roots of equation $g(s)=0$. To return from the complex variable s to the real variable in the determinant $\Delta^*(s)$, we write: $s=-\beta^2$ or $\sqrt{s}=i\beta$, where β is a real variable.

$$\begin{aligned}\Delta^*(s)\big|_{s=-\beta^2}&=\Delta_{12}(\gamma_{n+1}(s)L_n,\gamma_{n+1}(s)L_{n+1})\cdot\Delta'_{\overline{1,2n-1}}(s)-\Delta_{22}(\gamma_{n+1}(s)L_n,\gamma_{n+1}(s)L_{n+1})\cdot\Delta_{\overline{1,2n-1}}(s)\big|_{s=-\beta^2}=\\&=i^n\cdot\left[\delta_{12}(\varphi_{n+1}(\beta)L_n,\varphi_{n+1}(\beta)L_{n+1})\cdot\delta'_{\overline{1,2n-1}}(\beta)-\delta_{22}(\varphi_{n+1}(\beta)L_n,\varphi_{n+1}(\beta)L_{n+1})\cdot\delta_{\overline{1,2n-1}}(\beta)\right]\equiv i^n\cdot\delta(\beta)\end{aligned}\ ; \tag{41}$$

with:

$$\delta(\beta)=\delta_{12}(\varphi_{n+1}(\beta)L_n,\varphi_{n+1}(\beta)L_{n+1})\cdot\delta'_{\overline{1,2n-1}}(\beta)-\delta_{22}(\varphi_{n+1}(\beta)L_n,\varphi_{n+1}(\beta)L_{n+1})\cdot\delta_{\overline{1,2n-1}}(\beta)\,; \tag{42}$$

$$\gamma_k^2(s)\big|_{s=\beta^2}=-\Gamma_k\left(\frac{P_{\mathrm{inter}_k}}{3}\tau_{m_k}\beta^2+\left[1-\sqrt{\tau_{m_k}}\beta\cdot ctg\left(\sqrt{\tau_{m_k}}\beta\right)\right]\right)\equiv-\varphi_k^2(\beta);\quad\text{(from eq. (30))} \tag{43}$$

$$\begin{aligned}\Delta_{2j}(\gamma_k(s)L_{k-1},\gamma_k(s)L_k)&=i\cdot\left[v_{22}^{k-1,1}(\varphi_k(\beta)L_{k-1})\cdot v_{j1}^{k2}(\varphi_k(\beta)L_k)-v_{22}^{k-1,2}(\varphi_k(\beta)L_{k-1})\cdot v_{j1}^{k1}(\varphi_k(\beta)L_k)\right]\equiv\\&\equiv i\cdot\delta_{2j}(\varphi_k(\beta)L_{k-1},\varphi_k(\beta)L_k);\end{aligned}$$

$$\begin{aligned}\Delta_{\overline{1,2k-1}}(s)&=i^{k-1}\cdot\left[\delta_{11}(\varphi_k(\beta)L_{k-1},\varphi_k(\beta)L_k)\cdot\delta'_{\overline{1,2k-3}}(\beta)-\delta_{21}(\varphi_k(\beta)L_{k-1},\varphi_k(\beta)L_k)\cdot\delta_{\overline{1,2k-3}}(\beta)\right]\equiv\\&\equiv i^{k-1}\cdot\delta_{\overline{1,2k-1}}(\beta);\\\Delta'_{\overline{1,2k-1}}(s)&=i^{k-1}\cdot\left[\delta_{12}(\varphi_k(\beta)L_{k-1},\varphi_k(\beta)L_k)\cdot\delta'_{\overline{1,2k-3}}(\beta)-\delta_{22}(\varphi_k(\beta)L_{k-1},\varphi_k(\beta)L_k)\cdot\delta_{\overline{1,2k-3}}(\beta)\right]\equiv\\&\equiv i^{k-1}\cdot\delta'_{\overline{1,2k-1}}(\beta);k=\overline{2,n};\end{aligned}$$

$$\Delta_{\overline{1,1}}(s)=V_{11}^{11}(\gamma_1(s)L_1)=v_{11}^{11}(\varphi_1(\beta)L_1)\equiv\delta_{\overline{1,1}}(\beta);\Delta'_{\overline{1,1}}(s)=V_{21}^{11}(\gamma_1(s)L_1)=v_{21}^{11}(\varphi_1(\beta)L_1)\equiv\delta'_{\overline{1,1}}(\beta);$$

$$V_{1j}^{k1}(\gamma_m(s)L_k)=\cos\left[\varphi_m(\beta)L_k\right]\equiv v_{1j}^{k1}(\varphi_m(\beta)L_k)\,;V_{1j}^{k2}(\gamma_m(s)L_k)=i\cdot\sin\left[\varphi_m(\beta)L_k\right]\equiv i\cdot v_{1j}^{k2}(\varphi_m(\beta)L_k)$$

;

$$V_{2j}^{k1}(\gamma_m(s)L_k) = -\varphi_m(\beta)\cdot\sin[\varphi_m(\beta)L_k] \equiv v_{2j}^{k1}(\varphi_m(\beta)L_k);$$

$$V_{2j}^{k2}(\gamma_m(s)L_k) = i\cdot\varphi_m(\beta)\cdot\cos[\varphi_m(\beta)L_k] \equiv i\cdot v_{2j}^{k2}(\varphi_m(\beta)L_k); m = \begin{cases} k & ;j=1 \\ k+1 & ;j=2 \end{cases}.$$

According to Eq.(40), returning expression (37) to the original function gives:

$$C_k(t,Z) = \int_0^\infty \frac{1}{s\cdot\Delta^*(s)} W_{1,k}^*(s,Z)\cdot exp(st)\,dt =$$

$$= 1 + \sum_{j=1}^\infty \frac{W_{1,k}^*(s,Z)}{s\cdot\frac{d}{ds}\Delta^*(s)\Big|_{s=s_j}} exp(s_j t) = 1 - \sum_{j=1}^\infty \frac{W_{1,k}^*(\beta,Z)}{\beta^2\cdot\frac{d}{d\beta}\delta(\beta)\Big|_{\beta=\beta_j}} exp(-\beta_j^2\cdot t); \tag{44}$$

Calculation of the derivative $\frac{d\Delta^*(S)}{dS}$ of the determinant (41) is shown in appendix II.

According to the above computations, Eq. (39) is transformed:

$$W_{l,k}(\beta,Z) =$$

$$= \frac{1}{\delta(\beta)}\cdot\begin{cases} \prod_{j=1}^{n}\varphi_{j+1}(\beta)\cdot\cos[\varphi_1(\beta)Z] & ;k=1 \\ \prod_{j=k}^{n}\varphi_{j+1}(\beta)\cdot\left[\Phi_{22}^{k-1}(\varphi_k(\beta)L_{k-1},\varphi_k(\beta)Z)\cdot\delta_{\overline{1,2k-1}}(\beta) - \Phi_{12}^{k-1}(\varphi_k(\beta)L_{k-1},\varphi_k(\beta)Z)\cdot\delta'_{\overline{1,2k-1}}(\beta)\right] & ;k=\overline{1,n} \\ \left[\Phi_{22}^{n}(\varphi_{n+1}(\beta)Z,\varphi_{n+1}(\beta)L_{n+1})\cdot\delta_{\overline{1,2n-1}}(\beta) - \Phi_{12}^{n}(\varphi_{n+1}(\beta)Z,\varphi_{n+1}(\beta)L_{n+1})\cdot\delta'_{\overline{1,2n-1}}(\beta)\right] & ;k=n+1 \end{cases}. \tag{45}$$

Finally, we obtain the variation against time of the intercrystallite concentration *$C_k(t,Z)$* in the *k* layer at the position Z in the bed:

$$C_k(t,Z) = 1 + \sum_{j=1}^{\infty}\frac{exp(-\beta_j^2 t)}{\beta_j^2\cdot d\delta(\beta_j)}\begin{cases} \prod_{j=1}^{n}\varphi_{j+1}(\beta)\cos[\varphi_1(\beta)Z] & ;k=1 \\ \prod_{j=k}^{n}\varphi_{j+1}(\beta)\left[\Phi_{22}^{k-1}(\varphi_k(\beta)L_{k-1},\varphi_k(\beta)Z)\delta_{\overline{1,2k-1}}(\beta) - \Phi_{12}^{k-1}(\varphi_k(\beta)L_{k-1},\varphi_k(\beta)Z)\delta'_{\overline{1,2k-1}}(\beta)\right] & ;k=\overline{1,n}; \\ \left[\Phi_{22}^{n}(\varphi_{n+1}(\beta)Z,\varphi_{n+1}(\beta)L_{n+1})\delta_{\overline{1,2n-1}}(\beta) - \Phi_{12}^{n}(\varphi_{n+1}(\beta)Z,\varphi_{n+1}(\beta)L_{n+1})\delta'_{\overline{1,2n-1}}(\beta)\right] & ;k=n+1 \end{cases}$$

(46)

where $\beta_j, j=\overline{1,\infty}$ are roots of the transcendental equation:

Let us now write Eq. (28) in the form:

$$N_k^*(s,X,Z) = C_k^*(s,Z)\cdot\frac{sh\left[\sqrt{\tau_{m,k}s}X\right]}{sh\left[\sqrt{\tau_{m,k}s}\right]} \equiv C_k^*(s,Z)\cdot\omega_k^*(s,Z). \tag{47}$$

Then the expression of the Laplace original of expression (47) is conveniently computed applying the following formula [26]:

$$\tilde{\mathcal{L}}^{-1}[N_k^*(s,X,Z)] = \tilde{\mathcal{L}}^{-1}[C_k^*(s,Z)] * \tilde{\mathcal{L}}^{-1}[\omega_k^*(s,X)]\,. \tag{48}$$

$\tilde{L}$ = Laplace operator

Now we can calculate the original of expression $\omega_k^{\,*}(s,X)$:

$$\tilde{\mathcal{L}}^{-1}[\omega_k^*(s,X)] = \tilde{\mathcal{L}}^{-1}\Big[\frac{sh\sqrt{\tau_{m,k}s}\,X}{X\cdot sh\sqrt{\tau_{m,k}s}}\Big] = \sum_{j_1=0}^{\infty}\frac{sh\sqrt{\tau_{m,k}s}\,X}{X\dfrac{d}{ds}\Big[sh\sqrt{\tau_{m,k}s}\,\Big]_{s=s_{j_1}}}exp(s_{j_1}t)\,. \tag{49}$$

Here $s_{j_1} = -\dfrac{\pi^2 j_1^{\,2}}{\tau_{m_k}}, j_1 = \overline{0,\infty}$. are the roots of the equation $sh\sqrt{\tau_{m,k}s}$ =0.

Substituting $\sqrt{s} = i\beta$ or $s = -\beta^2$, we can obtain the original:

$$\omega_k(t,X) = \frac{2\pi}{\tau_{m,k}}\sum_{j_1=0}^{\infty} j_1(-1)^{j_1}\cdot\frac{sin(j_1\pi\cdot X)}{X}exp\Big(-\frac{j_1^{\,2}\pi^2}{\tau_{m,k}}t\Big); k = \overline{1,n+1}\,.$$

As the result of integration and simplification, we finally obtain at time t the diffusing gas concentration, $Q_k(t,X,Z)$, at a distance X (from the center) in the crystallites situated in the bed at the height Z from the bottom.

$$Q_k(t,X,Z) = \frac{2\pi}{\tau_{m,k}}\sum_{j_1=0}^{\infty} j_1(-1)^{j_1+1}\frac{sin(j_1\pi\cdot X)}{X\cdot\mu_{j_1}^2}\cdot$$
$$\cdot\left(1-exp\left(-\mu_{j_1}^2 t\right)\left[1-\sum_{j=1}^{\infty}\frac{\varepsilon_{j_1 j}(t)}{\beta_j^2\cdot d\delta\left(\beta_j\right)}\begin{cases}\prod\limits_{j=1}^{n}\varphi_{j+1}(\beta)\cdot cos\left[\varphi_1(\beta)Z\right] & ;k=1\\ \prod\limits_{j=k}^{n}\varphi_{j+1}(\beta)\begin{bmatrix}\Phi_{22}^{k-1}\left(\varphi_k(\beta)L_{k-1},\varphi_k(\beta)Z\right)\delta_{\overline{1,2k-1}}(\beta)-\\ -\Phi_{12}^{k-1}\left(\varphi_k(\beta)L_{k-1},\varphi_k(\beta)Z\right)\delta'_{\overline{1,2k-1}}(\beta)\end{bmatrix} & ;k=\overline{1,n}\\ \begin{bmatrix}\Phi_{22}^{n}\left(\varphi_{n+1}(\beta)Z,\varphi_{n+1}(\beta)L_{n+1}\right)\delta_{\overline{1,2n-1}}(\beta)-\\ -\Phi_{12}^{n}\left(\varphi_{n+1}(\beta)Z,\varphi_{n+1}(\beta)L_{n+1}\right)\delta'_{\overline{1,2n-1}}(\beta)\end{bmatrix} & ;k=n+1\end{cases}\right]\right); \tag{50}$$

where $\varepsilon_{j_1 j}(t)$ is :

$$\varepsilon_{j_1 j}(t) = \begin{cases}1-exp\left[-(\beta_j^2-\mu_{j_1}^2)t\right] & ;j_1\neq j\\ t & ;j_1 = j\end{cases}. \tag{51}$$

Appendix II

1) Calculation of the determinant $\Delta^*(s)$:

$$\Delta^*(s) = \Delta_{12}(\gamma_{n+1}(s)L_n,\gamma_{n+1}(s)L_{n+1})\cdot\Delta'_{\overline{1,2n-1}}(s) - \Delta_{22}(\gamma_{n+1}(s)L_n,\gamma_{n+1}(s)L_{n+1})\cdot\Delta_{\overline{1,2n-1}}(s)\,; \tag{52}$$

2) Calculation of the determinants $\Delta_{\overline{1,2k-1}}, \Delta'_{\overline{1,2k-1}}$:

$$\Delta_{\overline{1,1}} = V_{11}^{11}(\gamma_1 L_1); \Delta'_{\overline{1,1}} = V_{21}^{11}(\gamma_1 L_1);.$$

$$\Delta_{\overline{1,2k-1}} = \Delta_{11}(\gamma_k L_{k-1}, \gamma_k L_k) \cdot \Delta'_{\overline{1,2k-3}} - \Delta_{21}(\gamma_k L_{k-1}, \gamma_k L_k) \cdot \Delta_{\overline{1,2k-3}}; k = \overline{2,n}.$$

$$\Delta'_{\overline{1,2k-1}} = \Delta_{12}(\gamma_k L_{k-1}, \gamma_k L_k) \cdot \Delta'_{\overline{1,2k-3}} - \Delta_{22}(\gamma_k L_{k-1}, \gamma_k L_k) \cdot \Delta_{\overline{1,2k-3}}; k = \overline{2,n}. \; ; \qquad (53)$$

$$\Delta_{1j}(\gamma_k L_{k-1}, \gamma_k L_k) = V_{12}^{k-1,1}(\gamma_k L_{k-1}) \cdot V_{j1}^{k2}(\gamma_k L_k) - V_{12}^{k-1,2}(\gamma_k L_{k-1}) \cdot V_{j1}^{k1}(\gamma_k L_k) \; ;$$

$$\Delta_{2j}(\gamma_k L_{k-1}, \gamma_k L_k) = V_{22}^{k-1,1}(\gamma_k L_{k-1}) \cdot V_{j1}^{k2}(\gamma_k L_k) - V_{22}^{k-1,2}(\gamma_k L_{k-1}) \cdot V_{j1}^{k1}(\gamma_k L_k); j = \overline{1,2} \; . \qquad (54)$$

3) Calculation of derivative $\dfrac{d\Delta^*(S)}{dS}$ of determinant (41) :

$$\left.\frac{d\Delta^*(S)}{dS}\right|_{s=s_j} = i^n \cdot \frac{d}{d\beta} \delta(\beta)\Big|_{\beta=\beta_j} =$$

$$= i^n \left[\begin{array}{l} \frac{\partial}{\partial\beta}\delta_{12}\left(\varphi_{n+1}(\beta)L_n, \varphi_{n+1}(\beta)L_{n+1}\right)\delta'_{\overline{1,2n-1}}(\beta) + \delta_{12}\left(\varphi_{n+1}(\beta)L_n, \varphi_{n+1}(\beta)L_{n+1}\right)\frac{\partial}{\partial\beta}\delta'_{\overline{1,2n-1}}(\beta) - \\ -\frac{\partial}{\partial\beta}\delta_{22}\left(\varphi_{n+1}(\beta)L_n, \varphi_{n+1}(\beta)L_{n+1}\right)\delta_{\overline{1,2n-1}}(\beta) - \delta_{22}\left(\varphi_{n+1}(\beta)L_n, \varphi_{n+1}(\beta)L_{n+1}\right)\frac{\partial}{\partial\beta}\delta_{\overline{1,2n-1}}(\beta) \end{array} \right]_{\beta=\beta_j} \equiv i^n d\delta(\beta_j) \; ;$$

$$\frac{\partial}{\partial\beta}\delta_{\overline{1,2k-1}}(\beta) = \left[\begin{array}{l} d\delta_{11}\left(\varphi_k(\beta)L_{k-1}, \varphi_k(\beta)L_k\right)\delta'_{\overline{1,2k-3}}(\beta) + \delta_{11}\left(\varphi_k(\beta)L_{k-1}, \varphi_k(\beta)L_k\right)d\delta'_{\overline{1,2k-3}}(\beta) - \\ -d\delta_{21}\left(\varphi_k(\beta)L_{k-1}, \varphi_k(\beta)L_k\right)\delta_{\overline{1,2k-3}}(\beta) - \delta_{21}\left(\varphi_k(\beta)L_{k-1}, \varphi_k(\beta)L_k\right)d\delta_{\overline{1,2k-3}}(\beta) \end{array} \right] \equiv d\delta_{\overline{1,2k-1}}(\beta);$$

$$\frac{\partial}{\partial\beta}\delta'_{\overline{1,2k-1}}(\beta) = \left[\begin{array}{l} d\delta_{12}\left(\varphi_k(\beta)L_{k-1}, \varphi_k(\beta)L_k\right)\delta'_{\overline{1,2k-3}}(\beta) + \delta_{12}\left(\varphi_k(\beta)L_{k-1}, \varphi_k(\beta)L_k\right)d\delta'_{\overline{1,2k-3}}(\beta) - \\ -d\delta_{22}\left(\varphi_k(\beta)L_{k-1}, \varphi_k(\beta)L_k\right)\delta_{\overline{1,2k-3}}(\beta) - \delta_{22}\left(\varphi_k(\beta)L_{k-1}, \varphi_k(\beta)L_k\right)d\delta_{\overline{1,2k-3}}(\beta) \end{array} \right] \equiv d\delta'_{\overline{1,2k-1}}(\beta);.$$

$k = \overline{2,n};$

$$d\delta_{1j}\left(\varphi_k(\beta)L_{k-1}, \varphi_k(\beta)L_k\right) = dv_{12}^{k-1,1}\left(\varphi_k(\beta)L_{k-1}\right) \cdot v_{j1}^{k2}\left(\varphi_k(\beta)L_k\right) + v_{12}^{k-1,1}\left(\varphi_k(\beta)L_{k-1}\right) \cdot dv_{j1}^{k2}\left(\varphi_k(\beta)L_k\right) -$$
$$-dv_{12}^{k-1,2}\left(\varphi_k(\beta)L_{k-1}\right) \cdot v_{j1}^{k1}\left(\varphi_k(\beta)L_k\right) - v_{12}^{k-1,2}\left(\varphi_k(\beta)L_{k-1}\right) \cdot dv_{j1}^{k1}\left(\varphi_k(\beta)L_k\right);$$

$$d\delta_{2j}\left(\varphi_k(\beta)L_{k-1}, \varphi_k(\beta)L_k\right) = dv_{22}^{k-1,1}\left(\varphi_k(\beta)L_{k-1}\right) \cdot v_{j1}^{k2}\left(\varphi_k(\beta)L_k\right) + v_{22}^{k-1,1}\left(\varphi_k(\beta)L_{k-1}\right) \cdot dv_{j1}^{k2}\left(\varphi_k(\beta)L_k\right) -$$
$$-dv_{22}^{k-1,2}\left(\varphi_k(\beta)L_{k-1}\right) \cdot v_{j1}^{k1}\left(\varphi_k(\beta)L_k\right) - v_{22}^{k-1,2}\left(\varphi_k(\beta)L_{k-1}\right) \cdot dv_{j1}^{k1}\left(\varphi_k(\beta)L_k\right);$$

$$\frac{\partial}{\partial\beta}\delta_{\overline{1,1}}(\beta) = -L_1 \cdot d\varphi_1(\beta) \cdot \sin(\varphi_1(\beta)L_1) \equiv d\delta_{\overline{1,1}}(\beta);$$

$$\frac{\partial}{\partial\beta}\delta'_{\overline{1,1}}(\beta) = -d\varphi_1(\beta) \cdot \left[\sin(\varphi_1(\beta)L_1) - L_1 \cdot \varphi_1(\beta) \cdot \cos(\varphi_1(\beta)L_1)\right] \equiv d\delta'_{\overline{1,1}}(\beta);$$

$$\frac{\partial}{\partial\beta}v_{1j}^{k1}(\varphi_m(\beta)l_k) = -L_k \cdot d\varphi_m(\beta) \cdot \sin(\varphi_m(\beta)L_k); \; \frac{\partial}{\partial\beta}v_{1j}^{k2}(\varphi_m(\beta)L_k) = L_k \cdot d\varphi_m(\beta) \cdot \cos(\varphi_m(\beta)L_k);$$

$$\frac{\partial}{\partial\beta}v_{2j}^{k1}(\varphi_m(\beta)L_k)=-d\varphi_m(\beta)\cdot\left[\sin(\varphi_m(\beta)L_k)-L_k\varphi_m(\beta)\cos(\varphi_m(\beta)L_k)\right];$$

$$\frac{\partial}{\partial\beta}v_{2j}^{k2}(\varphi_m(\beta)L_k)=d\varphi_m(\beta)\cdot\left[\cos(\varphi_m(\beta)L_k)-L_k\varphi_m(\beta)\sin(\varphi_m(\beta)L_k)\right];$$

$$d\varphi_k(\beta)\equiv\frac{\partial}{\partial\beta}\varphi_k(\beta)=\frac{\beta\cdot\left[\frac{2P_{\mathrm{int}er,k}}{3}\tau_{m,k}-\sqrt{\tau_{m,k}}\cdot ctg\left(\sqrt{\tau_{m,k}}\beta\right)\right]-\frac{\tau_{m,k}}{\cos^2\left(\sqrt{\tau_{m,k}}\beta\right)}}{2\sqrt{1+\frac{P_{\mathrm{int}er,k}}{3}\tau_{m,k}\beta^2-\sqrt{\tau_{m,k}}\beta\cdot ctg\left(\sqrt{\tau_{m,k}}\beta\right)}};$$

$$\Phi_{ij}^k(\gamma_m(s)L_{k-1},\gamma_m(s)Z)=i\cdot\Phi_{ij}^k(\varphi_k(\beta)L_{k-1},\varphi_k(\beta)Z)\,.$$